



# XCHARM: A routing protocol for multi-channel wireless mesh networks



Kaushik R. Chowdhury<sup>a,\*</sup>, Marco Di Felice<sup>b</sup>, Luciano Bononi<sup>b</sup>

<sup>a</sup>Electrical and Computer Engineering Department, Northeastern University, Boston, MA 02115, USA

<sup>b</sup>Department of Computer Science, University of Bologna, Bologna 40127, Italy

## ARTICLE INFO

### Article history:

Received 12 July 2012

Received in revised form 17 May 2013

Accepted 1 July 2013

Available online 9 July 2013

### Keywords:

Cross-layer

Routing

Fading

Mesh networks

Interference

## ABSTRACT

Recent experimental results have pointed out the impact of physical layer multi-path fading and co-channel interference as the key factors influencing packet delivery among mesh routers (MRs) in wireless mesh networks. In addition, in a multi-channel environment, there exists significant power spectral overlap among channels used by MRs, leading to adjacent channel interference. In this paper, a cross-layer multi-radio, multi-channel routing protocol, XCHARM, is proposed in which the key contribution is the selection of the next hop, channel and transmission rate based on fading and interference concerns. The key features of our proposed protocol are as follows: (i) Routes are chosen based on the availability of channels that support high data rates, exhibit acceptable interference levels and long term resilience to fading related losses, (ii) The path latency is analytically calculated in advance for the candidate routes, accounting for channel induced errors, link layer contention, forward error correcting (FEC) codes, and the allowed data rates over the chosen channels, (iii) The route maintenance is performed by first attempting to identify and correct the point of failure before undertaking a global recovery action. An extensive performance evaluation, spanning the network, link and physical layers, reveals the benefits of adopting our cross-layer routing solution for wireless mesh networks.

© 2013 Elsevier B.V. All rights reserved.

## 1. Introduction

Wireless mesh networks (WMNs) allow supported mesh clients (MCs) to access the Internet gateway by multi-hop packet forwarding over the mesh routers (MRs) [4]. In this paper, we present XCHARM, a Cross-layer CHannel Adaptive Routing protocol for wireless mesh networks, that jointly addresses the concerns of interference, channel fading and transmission rate selection at the physical layer, and link layer error recovery, to meet the end-to-end user specified constraints.

In order to provide good network coverage and connectivity, the MRs are deployed in overlapping spatial regions, as shown in Fig. 1. The problem of interference due to simultaneous transmissions by other MRs, placed in close proximity of the receiver, has been shown to be a key problem in WMNs [17]. This may be alleviated to an extent by using multiple radios on different channels. However, this multi-channel environment introduces interference due to *spectral leakage* as the channels used by the MRs may not be completely non-overlapping. Due to concurrent transmissions on multiple channels and based on their separation in frequency, an additive effect may be seen in this spectral leakage power. The resulting high interference may render correct packet reception

infeasible for the considered link. In such cases, the routing protocol design becomes more involved, as interference prone regions, channel assignment and presence of multiple transceivers must also be considered in the route discovery process.

The physical phenomenon of multi-path fading has been shown to be an important reason for packet loss in WMNs [2]. Fading is mainly caused due to reflections from obstacles in the path between a given source–destination pair and results in a sudden, steep fall in signal strength. A type of fading, classified as *frequency selective*, affects the different frequency components of the signal to varying extents. This is particularly harmful as it requires complex hardware and equalizers rather than network protocol solutions for an acceptable packet reception rate. Thus, the routing protocol should be able to distinguish those channels that are preferable for transmission, and in the absence of any such channel, it should avoid the affected links altogether.

Apart from considering inter-channel interference and channel specific fading, classical routing protocols need further modifications before they can be used in a multi-channel environment. Consider the following case, in which, the route setup is undertaken using a common control channel (CCC) and the shortest path metric is used. In the classical AODV approach [25], the routing paths that deliver the route request message (RREQ) from the source first are selected at the destination. However, the RREQ propagates over the CCC, though the actual path uses entirely different channels for data transfer. Hence, its arrival time on the CCC

\* Corresponding author. Tel.: +1 6173735304.

E-mail addresses: [krc@ece.neu.edu](mailto:krc@ece.neu.edu) (K.R. Chowdhury), [difelice@cs.unibo.it](mailto:difelice@cs.unibo.it) (M. Di Felice), [bononi@cs.unibo.it](mailto:bononi@cs.unibo.it) (L. Bononi).

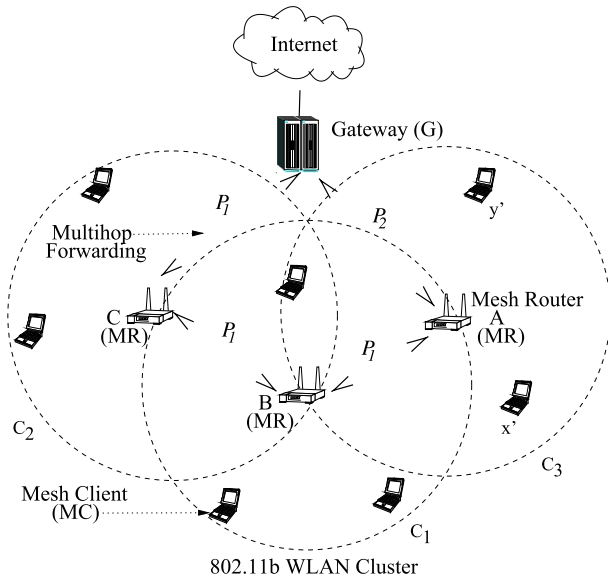


Fig. 1. The mesh network architecture.

is not indicative of the channel quality of the links that form the path. As shown in Fig. 1, the RREQ may arrive at the destination gateway through path  $P_2$  (A-G), earlier than path  $P_1$  (A-B-C-G), as it uses comparatively fewer hops. Thus, path  $P_2$  is chosen over path  $P_1$ , without considering the channel quality of the intermediate links that form the paths. A high packet error rate or a low permissible transmission rate, on the chosen channels for any of the links in the path  $P_2$ , may offset the advantage of creating shorter routes. There is, hence, a need to adapt the forwarding process of the RREQ, as function of the true channel quality of links that form the routing path. Additionally, several features of the link layer, such as forward error correcting (FEC) code bits, may also affect the data rate for the end-user.

XCHARM has been designed as a distributed routing protocol for WMNs that can address the above concerns by making the following key contributions:

- A interchannel interference model is proposed that accounts for spectral leakage between adjacent channels in a multi-channel scenario. The task of channel selection and estimation of the fading environment is integrated in the proposed routing scheme.
- An analytical expression for the end-to-end latency is derived, that accounts for the error due to the physical environment and link layer decisions of FEC code length.
- A route management functionality is proposed that continuously monitors the performance of the route and initiates local recovery actions by identifying the particular link that causes the bottleneck in the route.

The preliminary findings of this work were published in [8]. In this paper, we have expanded our work significantly by adding an experimental study as motivation, integrating link layer FEC selection, proposing analytical expressions for path latency, enhancing the performance evaluation by comparison with existing schemes, and route management techniques.

The rest of this paper is organized as follows. Section 2 describes the related work and motivates the need for a new cross-layer fading-aware routing scheme. In Section 3, our proposed protocol is described. A thorough performance evaluation is conducted in Section 4. Finally, Section 5 concludes our work.

## 2. Related work and motivation

In this section, we review cross-layer routing protocols for mesh networks that are chiefly concerned with meeting delay requirements, rather than energy consumption [4].

### 2.1. Related work

For single channel networks, centralized protocols formulate the task of joint route selection, link level scheduling, and power control [3] as an optimization problem. This can then be solved when the constraints of packet generation at the source and the total traffic arriving at the destination are known [20]. Recently, a routing algorithm considering the network, link and physical layers and also end-to-end constraints is proposed in [10]. However, modeling link access delay is non-trivial. The assumption of the random link delay in [10], and the TDMA scheduling in [20] integral to the linear programming formulation, restrict the applicability of such works for practical mesh networks. This limitation is also common to the distributed approaches presented in [16].

Unlike single-channel cross layer protocols discussed above, the use of multiple channels helps in increasing the system throughput by using the available spectrum efficiently. The problem of joint channel assignment and routing based on flow fairness is addressed through centralized approaches, in which, the complete knowledge of the flows between any two MRs is known [5]. Here, a network-wide optimization problem is solved and a constant factor approximation to the optimal solution is provided. These two goals are also considered in the distributed scheme in [19]. When the traffic demands of the flows are not known in advance, an estimation on the mean value and the statistical distribution based on the prior history is undertaken in [14]. A similar joint routing and scheduling approach in [12], lacks physical layer considerations that are present in our work. These works, however, do not scale well with node density owing to the centralized nature of the solution.

In many existing works, distributed routing protocols for multi-channels multi-radio WMNs are extensions of classical wireless ad hoc routing schemes [9]. In [26], the Multi-Radio Ad Hoc On-Demand Distance Vector (AODV-MR) is proposed, by extending the popular AODV [25] routing protocol in a multi-radio environment, though the channel selection is performed randomly during the route discovery phase. The Load-Aware Routing Protocol (LMR) [22] extends the AODV-MR [26] scheme with a channel selection scheme which takes into account the traffic load of each channel. Different from these approaches, a mechanism for automatic rate selection and route quality evaluation using statistical information (instead of instantaneous channel measurements) is proposed in [24]. Other recent works tradeoff throughput for interference protection to the flows during path selection [6], while the reverse consideration is present in [15].

In using packet error as the main metric, some links may not be preferred for a route owing to errors caused by reasons such as: contention losses, buffer overflow etc. However, in a cross-layer approach, such as ours, these can be identified and corrective actions can be taken at that specific underlying layer. Instead, we wish to explore certain unique environmental conditions that are out of control of the node (say, reflections that cause frequency selective fading), which have severe and long term impact on routing, and must be avoided right at the onset.

In XCHARM we adopt a cross-layered design which allows to (i) distinguish the type of fading on each link, so that flat-fading links offering high data-rates are preferred (Section III.C) (ii) allocate channels among the flows in a distributed way in order to minimize the interference caused to other MRs transmitting on other

(possibly non-orthogonal) channels (Section III.B) and (iii) select routes based on performance requirements of the application, and provide mechanisms for route performance monitoring and re-routing in case such requirements are no longer satisfied (Sections III.D and III.E).

2.2. Motivation

A key contribution of our work is proposing a new route metric based on the fading characteristics of the channel, the impact of which is described in the experimental evaluation in this section. Recent experiments carried out in [2] point out fading to be an important cause for packet loss in WMNs. Fading can be classified into flat or frequency selective based on the coherence bandwidth ( $B_c$ ) of the channel.  $B_c$  is defined as the approximate maximum bandwidth over which two frequencies of a signal are likely to experience comparable amplitude fading. If the coherence bandwidth of the channel ( $B_c$ ) is lesser than the signal bandwidth, frequency selective fading is observed. This is particularly harmful as various frequency components are affected differently and requires complex hardware, such as RAKE receivers with multiple taps. If  $B_c$  is greater than the signal bandwidth, it results in a flat fading channel. Here, the signal experiences fluctuations with time with occasional deep fades, but shows a constant channel gain in the frequency domain. The bit error rate (BER) using QPSK modulation, for these two types of fading is shown in Fig. 2(a). It shows

the high PER for the case of frequency selective fading, thus motivating the need to identify such links and avoid their assimilation in the routes. While the existing literature has focused on varying transmission power, rate and channel interference at the physical layer, fading has not yet been considered as a routing metric.

The experiment involved placing two laptops at locations A and B in a residential setting, equidistant from an access point (AP), transmitting at a constant rate of 1 Mbps. Both laptops used similar IEEE 802.11b NETGEAR MA401 wireless cards, but location A was chosen such that there were several man-made obstructions on the signal path from the AP. Interfering wireless sources were identified and contained for the duration of the experiment with the help a spectrum analyzer. This method of using a spectrum analyzer was preferred over calculating the noise floor through the received signal strength (RSS) values just before the packet reception by WLAN cards on the laptop. This eliminates the variability seen in the detection times on the WLAN card in the laptops used for the experiment, as pointed out in [17], and in turn improves the accuracy of the noise estimation which we measured at  $-100$  dBm.

We observe from Fig. 2(b) and (c), that the average received signal strength (RSS) was similar ( $-79.598$  and  $-79.35$  dBm) though location A suffered a high packet error rate (PER). Thus, the RSS and the signal to noise plus interference ratio (SINR) derived from it, did not reflect the observed trend in the PER at A. This was because, in the known interference environment, though the RSS measurements had the same mean, there was considerably more

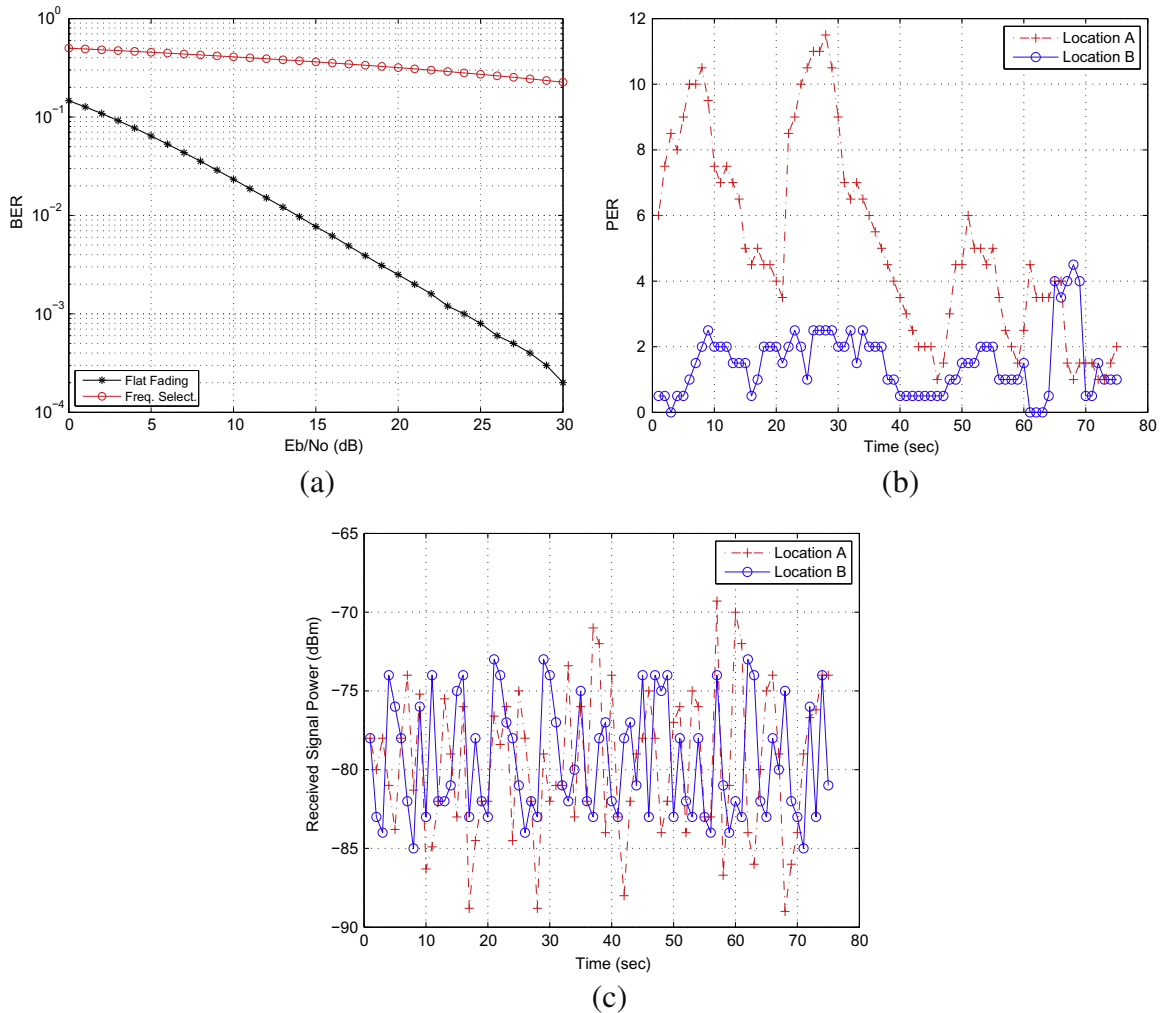


Fig. 2. The theoretical BER for flat and frequency selective fading as a function of SNR is plotted in (a). The PER (b) and RSS (c) are shown for our experiment.

signal variance at location  $A$  due to the arrival of multi-path components with different path gains.

The fading properties of a link can be identified by directly measuring the packet error rate over time. However, we assume that links may not be active before formation of the routes, and hence MRs cannot collect the PER statistics in advance. As a contrast to this approach, a channel sounding technique based on pulse transmissions is integrated in the XCHARM. Here, pilot pulses are sent out and the fading estimate is obtained by measuring the delay spread of their arrival times [21]. This delay spread can be inverted to give the coherence bandwidth  $B_c$ .

### 3. XCHARM: a cross-layer routing protocol

Our reference WMN architecture is shown in Fig. 1. Several MCs, possibly mobile, may be under the coverage of a stationary MR. The MRs form the wireless backbone for carrying data flows to and from the MCs by multi-hop forwarding to reach the Internet gateway. XCHARM provides a solution for the MR-MR routing and is assumed to operate on channels not affected by the MR-MC traffic [4]. A CCC is used during route setup, though the MR is equipped with multiple transceivers, each of which can operate independently in different channels. We consider the legacy IEEE 802.11b standard [1] at the link layer. In addition, assume that the available channels are half-duplex, supporting multiple transmission rates,  $T_1 < \dots < T_\psi$ , that require bandwidth  $B_1 < \dots < B_\psi$  respectively. These can be obtained from the Shannon's capacity limit [18] after suitable standard-specific scaling factors are assumed.

XCHARM comprises of the following six functions: (i) Channel selection stage, in which, the MR forwarding the RREQ and its potential next hops decide on a set of usable channels while accounting for external interference, (ii) Channel and MR ranking, that establishes an order of preference in the channels and the candidate forwarding MRs, that are found to be suitable for transmission, (iii) Defer Timer, that helps in forming good routes by deferring the forwarding process at the MRs as a function of their ranks, (iv) FEC assignment, that decides in part the end-to-end performance of the routes, (v) Route selection by the destination, and (vi) Route management to ensure the feasibility of the route. We first give an overview of the working of our protocol and then describe each stage in detail.

#### 3.1. Protocol overview

XCHARM uses an on-demand routing approach, inspired by the AODV protocol [25]. The route discovery procedure is invoked only when a route between a new source–destination pair should be established. In such a case, the RREQ is sent out by the source MR on the CCC. In this packet, the MR also includes the list of channels that are *favorable* to it. The *favorable* set of channels is so chosen that the other receivers in its transmission range are not affected when the new route is in use. On this set of channels, the transmitting MR also emits pilot pulses, so that the receiver MRs can estimate the channel quality, based on the discussion on fading estimation in Section 2.2. This RREQ is received by several potential next-hop MRs, which then check their own interference neighborhood to identify a set of mutually acceptable channels, called as the *favorable* channel set. From the receiver's viewpoint, the channels chosen by it should not be susceptible to interference from other transmitters in its vicinity. Each receiver then proceeds to preferentially order the set of favorable channels, based on the pulse based fading estimation and the maximum allowed transmission rate. At the same time, from the strength of the received pulses on the acceptable channels, it can estimate the FEC

length that would be needed to keep the packet error below a pre-decided threshold.

We introduce a ranking function that allows the receiver MRs to rank themselves on an absolute scale, based on the best channel that they perceive. This can also be considered as choosing which MR is the most suitable next hop forwarder for the RREQ, as a function of the link channel characteristic. The MRs defer the propagation of the RREQ depending on their ranks and this ensures that at each link, the MRs with the best channel quality get transmission priority. While forwarding the RREQ, the MR also includes in it, the value of the FEC and also an analytical estimation of the expected link delay on the chosen channel. This process is repeated for the intermediate hops and finally the destination uses the information in the arriving RREQ packet to check if the user specified end-to-end constraints are met. If so, the route reply (RREP) message is sent back to the source. Consider the MR  $i$  that forwards the RREP message to next-hop MR, say MR  $j$ , in which the former node includes the channel previously chosen for link  $i$ – $j$ . When MR  $j$  receives the RREP message, before forwarding it, it broadcasts a Channel Confirmation message (CCONF) to inform other neighbouring MRs about the channel allocation. The CCONF message includes (i) the channel chosen on link  $i$ – $j$ , (ii) the  $ID$  and location of the transmitter node (i.e., MR  $i$ ), and (iii) the  $ID$  and location of the receiver node (i.e., MR  $j$ ). The CCONF message is received by all the neighbours of MR  $j$ , and it is re-broadcast by other MRs for a maximum number of hops  $h$ . In our work, we set  $h$  equal to 2. In this way, all nodes at 2-hop distance of current receiver/transmitter nodes are informed about the channel allocation performed by MR  $i$  and MR  $j$  and their locations. The RREP forwarding is continued till the source is discovered. Then, the route is established and can be used to transmit data packets.

In addition, the MRs along the chosen route as well as the destination monitor the route continuously. If the performance constraints are not satisfied for a fixed duration due to change in the network environment, the affected location is identified, and a route error (RERR) message is sent for possible new route discovery. The old route is kept in operation till a new one is identified, after which it is torn down by the RTEAR message and the committed resources are reclaimed by the intermediate MRs.

#### 3.2. Channel selection stage

The main functionality of this stage is to ensure that the sender and receiver MR pair agree on a channel, such that, the effect of external interference on it is minimized. In addition, when this channel is used for transmission, it should not adversely affect the ongoing communication in the neighborhood. We first define our interference model and then propose our channel selection algorithm.

##### 3.2.1. Interference model

In a multichannel environment, the assumption of strictly non-overlapping channels may not be correct. As an example, significant power leakage between adjacent channels occurs in the IEEE 802.11b systems. Our protocol determines channel availability based on the summation of the individual leakage powers in that channel. We assume a simple free space path loss model and a constant transmit power for all MRs, normalized to 1. Now, the average power,  $P_{ij}(f_i, f_j)$ , received on channel  $f_j$  at MR  $j$  due to transmitter MR  $i$  on channel  $f_i$ , when separated by a distance  $D_{ij}$  is given by,

$$P_{ij}(f_i, f_j) = I(f_i, f_j) \cdot \alpha_i D_{ij}^{-\beta} \quad (1)$$

Here,  $\alpha_i = \frac{G_t G_r c^2}{(4\pi f_i)^2}$ , where  $G_t$  and  $G_r$  are the transmit and receiving antenna gains, and  $c$  is the speed of light.  $I(f_i, f_j)$  is the spectral overlap

factor or the leakage power between the channels of transmitter ( $f_i$ ) and receiver ( $f_j$ ). This is either made available as standard data based on channel separation or can be calculated through power mask requirements [23].

Our proposed approach allows the MRs to use more than one transceiver for sending and receiving data packets concurrently. However, each transceiver must be tuned to a different half duplex channel. A given MR  $i$  maintains a list of channels that it is currently using for data transmission ( $C_i^T$ ) and reception ( $C_i^R$ ). These sets are periodically communicated to the other MRs within transmission range by the exchange of beacon messages. Further, let  $S_i^R$  and  $S_i^T$  represent the MRs within range of MR  $i$ , that are currently receiving and transmitting respectively on at least one channel. As an example, for MR  $B$  in Fig. 3, we have  $S_B^R = \{D\}$ ,  $S_B^T = \{A, C\}$ ,  $C_B^R = \{4\}$ ,  $C_B^T = \phi$ . Also,  $C_A^T = \{3, 6\}$ . In our solution,  $S_i^T$  and  $S_i^R$  are dynamically built by MR  $i$ , by means of the following messages:

- CCONF message: each CCONF message contains a channel allocation (say channel  $x$ ), the location and  $id$  of the sender node (say  $s_c$ ), the location and  $id$  of the receiver node (say  $r_c$ ). On receiving the CCONF message, MR  $i$  will include  $s_c$  in  $S_i^T$  and  $r_c$  in  $R_i^T$ . Since these messages are re-broadcasted by neighbors of current sender and receiver nodes, this means each MR  $i$  might take into account channel selection performed by other MRs at 1 and 2 hops of distance, in order to mitigate *inter-flow* interference problems.
- RREQ message: in this case, MR  $i$  is aware of previous MRs (e.g.,  $\{MR_{RREQ}\}$ ) traversed by the RREQ message. Then, it will include all the nodes belonging to  $\{MR_{RREQ}\}$  in  $S_i^T$  and  $R_i^T$ . This means MR  $i$  takes into account channel selection performed by other MRs in the same route, in order to mitigate *intra-flow* interference problems.

### 3.2.2. Channel selection

In the overview of our scheme, we used the term *favorable* to describe the set of channels,  $F_i^T$  and  $F_j^R$ , that may be preferred at the sender, say MR  $i$ , and the receiver, say MR  $j$  respectively. The set  $F_j^R$  is created as a subset of  $F_i^T$ , such that there is at least one common channel that is acceptable to both the MRs of a given link. We can formally define these sets as follows,

**Definition 1** (*Favorable transmitter set ( $F_i^T$ )*). This is a set of channels, such that, when MR  $i$  uses any of them for transmission, an acceptable interference power is introduced in the channels used for reception by the other MRs in its range.

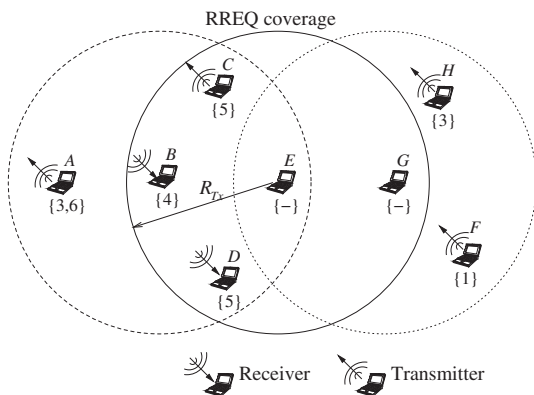


Fig. 3. RREQ coverage area and formation of favorable sets at the transmitter and receiver. The channels used by an MR are indicated in the parenthesis.

**Definition 2** (*Favorable receiver set ( $F_j^R$ )*). This is a set of channels chosen by the MR  $j$ , as a subset of the received set  $F_i^T$ , such that, for each channel the total interference is within an acceptable level.

The word *acceptable* implies that the measured interference power is below a pre-decided threshold necessary for correct packet reception. We next describe how these sets are constructed and their role in the interference management of a link.

A given MR  $j$  experiences a finite amount of total interference power,  $P_j^I(f_j)$  on each of these channels  $f_j \in C_j^R$  due to spectral leakage from all the transmitting MRs,  $S_j^T$ , in the vicinity. The total interference on a channel  $f_j$ ,  $P_j^I(f_j)$ , can be expressed using Eq. (1),

$$P_j^I(f_j) = \sum_{\forall k \in S_j^T, f_k \in C_k^T} P_{kj}(f_k, f_j) \quad (2)$$

Thus, from Fig. 3,  $B$  receives a finite interference power on channel 4 given by  $P_B^I(4) = P_{A,B}(3, 4) + P_{C,B}(5, 4)$ .

When the MR  $i$  forwards an RREQ, it first creates its favorable set  $F_i^T$ . The transmitted power on any channel  $f_j \in F_i^T$  adds to the interference in the channels used by a neighboring MR  $j$  for reception ( $C_j^R$ ). This additional injected power should not cause the interference level to rise higher than the allowed threshold  $P_{th}$ . This condition is checked for all the active receivers in the transmission range of MR  $i$ , i.e.,  $j \in S_i^R$ . Using Eq. (2), we can formally express the favorable transmitter set,  $F_i^T$  as,

$$F_i^T = \{f_i | P_{ij}(f_i, f_j) < P_{th} - P_j^I(f_j), \forall j \in S_i^R, f_j \in C_j^R\} \quad (3)$$

From Fig. 3, MR  $E$  is in the process of forwarding the RREQ and must create the set  $F_E^T$ . Active receivers in its range are  $R_E = \{B, D\}$  and the respective reception channel sets are  $C_B^R = \{4\}$  and  $C_D^R = \{5\}$ , respectively. MR  $E$  may include the channel 7 in  $F_E^T$  only if the conditions  $P_{E,B}(7, 4) < P_{th} - P_B^I(4)$  and  $P_{E,D}(7, 5) < P_{th} - P_D^I(5)$  are satisfied.

On receiving the set of favorable channels ( $F_i^T$ ) from the transmitting MR  $i$ , the candidate next hop MRs form their favorable receiver set ( $F_j^R$ ) which, by Definition 2, is acceptable to both the sender and receiver on the link. Thus,

$$F_j^R = \left\{ f_j \left| \sum_{\forall k \in S_j^T, f_k \in C_k^T} P_{kj}(f_k, f_j) < P_{th}, f_j \in F_i^T \right. \right\} \quad (4)$$

In our example, we assume that MR  $G$  received an RREQ from  $E$ , containing  $F_E^T = \{2, 7\}$ . The active transmitters in its receiving range form the set,  $S_G^T = \{F, H\}$ . The channel 2 may not be chosen by MR  $G$ , as it may see large spectral leakage from the adjacent channels 1 and 3 used by MRs in its vicinity. Noting that  $F_G^R \subseteq F_E^T$ , if channel 7 has an aggregate interference power less than the threshold, i.e.,  $P_{F,G}(1, 7) + P_{H,G}(3, 7) < P_{th}$ , then  $7 \in F_G^R$ .

The main goal of our channel allocation scheme is to maximize the frequency reuse, by allocating different flows on non co-interferer channels. However, it is possible that no mutually acceptable channel is found for a given pair of MRs  $i$  and  $j$ , because all the channels have already been allocated in the neighbourhood. Thus, if  $F_j^T = \phi$  or a non-empty favorable set at the transmitter gives  $F_j^R = \phi$  at the receiver, it implies that the interference on the link, or caused by it is unacceptable. In this case, the receiver MR  $j$  chooses the minimum interference channel, i.e., the channel for which  $P_j^I(f_j)$  is minimum. The MR  $j$ , however, flags this condition and imposes a stiff forwarding penalty on itself, as we shall see in Section 3.3.3.

In the general case, the RREQ is received by several candidate forwarders, each having more than one suitable channel for the link. In the next step, we introduce a *ranking* concept that helps in choosing, a particular channel and the MR that shall forward

the RREQ earlier than the others. This procedure also accounts for channel fading and biases the formation of routes with better quality links.

### 3.3. Channel and MR ranking

We recall that the MR  $i$  that forwards the RREQ, also sends out pilot pulses in the channels of its favorable set  $F_i^r$ . We first describe how this is achieved at the link layer and the subsequent methodology. A ranking concept is then devised based on the maximum allowed transmission rate of a channel that can be supported in the fading environment.

#### 3.3.1. Pilot pulse transmission

We recall that a transceiver, in a given MR, can be set at one of the  $\psi$  different transmission rates, corresponding to the  $\psi$  allowed signal bandwidths. When the MR attempts to send out the channel sounding pulses, it is possible that MR  $i$  senses the channel busy, and so it is forced to delay the transmission of the pulses. Also, the receiver may miss the pulses altogether due to external interference or an ongoing data transaction on these channels. These conditions are shown in channels  $f_1$  and  $f_2$ , respectively (Fig. 4), resulting in a deaf period at the receiver. XCHARM partly addresses this problem by preferential transmission of the pulses over other data packets. It allows an MR to capture the channel by waiting for an interval given by the Short Inter-Frame Spacing (SIFS), when the channel is sensed free, as against the larger Distributed Inter-Frame Spacing (DIFS) used for normal packets. In Fig. 4, MR  $i$  seizes the channels  $f_1$  and  $f_2$ , after an SIFS duration, from the moment they become available. The receiver can only consider those channels for creating its own favorable set in which it receives the pilot pulses.

#### 3.3.2. Fading and rate estimation

The fading estimate of a given channel  $f_j \in F_j^R$  is obtained by the receiver MR  $j$ , by measuring the delay spread of the arrival times of the pilot pulses, as described in Section 2.2. This delay spread is inverted to get the coherence bandwidth ( $B_c^f$ ), for each channel  $f_j$  in the favorable receiver set. Also, we recall that  $B_1, \dots, B_\psi$  are the different signal bandwidths possible, each  $B_k$  resulting in a maximum transmission rate  $T_k$ . We next order the channels and the MRs based on these maximum allowed transmission rate.

#### 3.3.3. Rank assignment

The rank of a given channel is defined formally as:

**Definition 3** (Channel rank ( $r_{ij}^{ch}(f_j)$ )). For the transmitter  $i$  and receiver  $j$  pair, this is the index  $k$  of the highest transmission rate for transmitter  $i$  allowed by the receiver  $j$ ,  $T_k$ , such that the channel  $f_j$  is flat fading.

Thus,

$$r_{ij}^{ch}(f_j) = \arg_k \max [T_k | B_k < B_c^f]. \quad (5)$$

We recall that, if the coherence bandwidth of the channel ( $B_c^f$ ) is greater than the bandwidth used for the signal ( $B_k$ ), then the channel is flat fading. Thus Eq. (5) attempts to find out that flat fading channel ( $B_k < B_c^f$ ) in the favorable set of the receiver, such that the highest possible transmission rate ( $T_k$ ) is supported. The channel rank  $r_{ij}^{ch}(f_j)$  takes the index of the this maximum possible rate, for a given channel  $f_j \in F_j^R$ .

From Section 2.2, if the order relation between the signal bandwidths and channel coherence bandwidth is  $B_1 < B_2 < B_c^f < B_3 < \dots < B_\psi$ , then the channel  $f_j$  is flat fading for  $B_1$  and  $B_2$ , but frequency selective for the rest. Hence, if this channel is chosen for

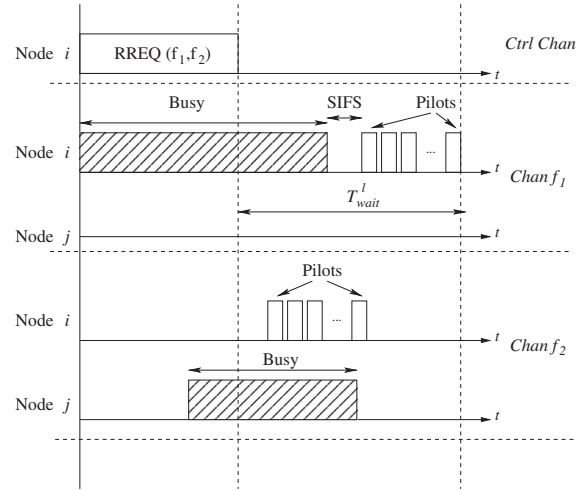


Fig. 4. The pilot pulses are transmitted on the channels specified by the RREQ, sent over the CCC.

the link between two MRs, the transmission rate at the previous hop  $i$  must be  $T_2$  (based on the condition  $B_2 < B_c^f < B_3$ ). This gives the highest allowed transmission rate ( $T_{max}^f$ ) on channel  $f_j$  while keeping the flat fading characteristics. Thus, the channel rank  $r_{ij}^{ch}(f_j) = 2$ , as  $T_{max}^f = T_2$ .

On similar lines, we define the MR rank as:

**Definition 4** (MR rank ( $r_{ij}^{MR}$ )). For the transmitter–receiver pair  $i - j$ , the rank of the potential next hop MR  $j$  is the maximum channel rank over all the channels  $f_j$  in its favorable receiver set,  $F_j^R$ .

Thus,

$$r_{ij}^{MR} = \max \{ r_{ij}^{ch}(f_j), \forall f_j \in F_j^R \}. \quad (6)$$

The rank of a MR helps in classifying the potential next-hops based on (i) whether the channel is feasible for transmission based on fading, and (ii) the maximum transmission rate that is possible on that channel. We next introduce a forwarding delay through a defer timer (DT) based on MR ranks. Here, the MR with the smaller rank will defer its forwarding of the RREQ for a longer time as compared to the MR with the higher rank. Thus, this allows the route information formed by higher ranked MRs to be received earlier at the destination.

### 3.4. Defer timer

Let the maximum time that an MR can defer forwarding the RREQ be the system parameter  $T_{max}^{def}$ . As the MR rank can take  $\psi + 1$  values from  $0, \dots, \psi$ , we divide this interval into  $\psi + 1$  sub-intervals, each of duration  $\frac{T_{max}^{def}}{(\psi + 1)}$  units. An MR  $j$  defers the RREQ received from a sender, say  $i$ , for a duration that is an integral multiple of this unit. Intuitively, in the candidate set of forwarders  $j$  and  $l$ , if MR  $j$  has the highest possible rank ( $r_{ij}^{MR} = \psi$ ), it should have minimum forwarding delay. On the other hand, MR  $l$  has only frequency selective channels ( $r_{il}^{MR} = 0$ ). It is not preferred as the next hop, and must defer for the longest time. This behavior is captured by the following defer timer that returns the total delay  $F_{ij}$  towards forwarding the RREQ received from MR  $i$  at MR  $j$ ,

$$F_{ij} = \left\{ \frac{T_{max}^{def}}{(1 + \psi)} \cdot (\psi - r_{ij}^{MR}) \right\} \cdot \kappa, \quad (7)$$

where

$$\kappa = \begin{cases} 1 + \psi & \text{if } F_j^R = \phi, \\ 1 & \text{otherwise.} \end{cases}$$

In the above expression,  $\kappa$  is a weighting factor that is decided on the basis of the feasible receiver set,  $F_j^R$ . If at least one mutually acceptable channel is found,  $\kappa = 1$ . This ensures that the forwarding delay at the MR  $j$  is purely a function of its channel ranks (and hence the fading environment). However, if no common channel exists between the sender and receiver, given by  $F_j^R = \phi$ , any one channel may be chosen by the receiver (from Section 3.2.2). In this case, the forwarding delay at the MR  $j$  is significantly increased, to a multiple of the maximum deferring time  $T_{\max}^{\text{def}}$ , by the factor  $\kappa = (1 + \psi)$ . Thus, routes that pass through this link may be formed with the least priority. In the example above, MR  $j$ , with a better channel between itself and MR  $i$ , can immediately forward the RREQ packet to its link layer buffer as  $F_{ij} = 0$ . Conversely, MR  $i$  must wait for the duration of  $F_{ii} = \frac{\psi}{T_{\max}^{\text{def}}}$  units.

Traditional routing metrics, such as minimum hop count or distance from the destination, can be linearly combined with our fading-based deferring time. We achieve this by extending Eq. (7) as,

$$F_{ij} = \frac{T_{\max}^{\text{def}}}{(\psi + 1)} \cdot \left\{ \frac{W_1}{W_1 + W_2} \cdot (\psi - T_{ij}^{\text{MR}}) + \frac{W_2}{W_1 + W_2} \cdot X \right\} \cdot \kappa, \quad (8)$$

where  $W_1$  and  $W_2$  are the user-specified weights,  $\psi$  is the total number of allowed transmission rates and  $X$  denotes the combination of the other classical metrics that need to be incorporated. The only constraint in specifying  $X$  is that the best value of the metric is indicated by 0 and the worst case by  $\psi$ . However, owing to space constraints in this paper, we limit the subsequent discussion to the MR rank metric only, i.e., we assume  $W_2 = 0$  and the results can be trivially extended to the general case.

In summary, the purpose of the defer timer is to prefer links with flat fading characteristics that can support the highest transmission rates. However, from Fig. 2(a), we observe that flat fading links also experience bit errors based on the value of the received SNR. The resulting packet loss can be mitigated by the use of an appropriate FEC at the link layer, and we show next how this selection determines the end-to-end performance of the chosen route.

### 3.5. Routing performance With FEC codes

The FEC bits added to the data payload help in reducing the packet losses due to bit errors. This, in turn, results in fewer re-transmissions at each link and reduced link and end-to-end delays. At the same time, the FEC bits constitute an overhead by increasing packet sizes, lowering channel utilization and reducing the useful bits arriving per unit time at the destination.

In this work, we assume Reed–Solomon (RS) codes for the link layer FEC motivated by its simplicity in implementation, widespread use and to ensure a tractable analysis. We consider the following end-to-end metrics:

1. Path Latency ( $L_\eta$ ): This is defined as the total expected time from packet creation at the source to reception at the destination for a path  $\eta$ . This is the summation over the delay experienced at each node  $i$  of the path ( $T_i^D$ ).
2. Goodput ( $G_\eta$ ): This metric measures the number of useful bits delivered per unit time by the path  $\eta$ . It is decided by the choice of FEC for the bottleneck node  $j$  in the route, and is the ratio of the data bits in a packet to the hop delay,  $T_j^D$ , at that node.

RS codes can be expressed concisely in the form  $(n, k)$ . Here,  $n$  is the block length in bytes,  $k$  gives the data payload and the code can correct up to  $t(k) = \frac{n-k}{2}$  bytes in a given block. By keeping the packet size  $l$  and the block size  $n$  fixed, we can express the FEC as a function

of the single unknown  $k$ . We next derive expressions for each of these metrics, as a function of the link FEC ( $k$ ).

#### 3.5.1. FEC influencing path latency

From the definition of path latency and for a path  $\eta$  of  $H_\eta$  hops,

$$L_\eta = \sum_{i=0}^{H_\eta} T_i^D \quad (9)$$

The total analytical hop delay,  $T_i^D$ , incurred at node  $i$  is the sum of the buffer latency,  $T_i^{\text{buf}}$ , and the transmission delay,  $T_i^{\text{acc}}$ , for the channel chosen by the receiver. Thus,

$$T_i^D = T_i^{\text{buf}} + T_i^{\text{acc}} \quad (10)$$

$T_i^{\text{acc}}$  is the average time taken by an MR to successfully transmit a packet, while accounting for the channel access time at the link layer, the probability of successful transmission and the rate at which the data bits are placed on the channel. As we consider the 802.11b standard which is a contention-based protocol, let  $W$  be the minimum contention window,  $m$  is the number of allowed retries,  $\tau$  is the probability of transmission in a slot,  $N_i$  is the number of transmitting MRs in the neighborhood of MR  $i$ , and  $E[\text{slot}]$  is the average length of the slot time [7]. Assuming that all transmitting MRs are in saturation,  $T_i^{\text{acc}}$  is obtained in [11] as,

$$T_i^{\text{acc}} = \sum_{\mu=0}^m \left[ \frac{W_\mu + 1}{2} \cdot \frac{p^\mu - p^{m+1}}{1 - p^{m+1}} \right] \cdot E[\text{slot}] \quad (11)$$

where,  $p$  is the probability that a packet drop can be dropped (i) due to collision or (ii) channel error caused by fading and is calculated as,

$$p = 1 - (1 - \tau)^{N_i - 1} \cdot (1 - \text{PER}(k_i)) \quad (12)$$

For a packet of  $l$  bytes, there are a total of  $\lceil \frac{l}{n} \rceil$  blocks. The packet is considered to be in error even if one of its consequent blocks cannot be recovered by the FEC ( $k_i$ ), with say, probability  $p_{bk}(k_i)$ . Thus, the PER( $k_i$ ), as a function of the FEC, is given by,

$$\text{PER}(k_i) = 1 - (1 - p_{bk}(k_i))^{\lceil \frac{l}{n} \rceil} \quad (13)$$

The block error probability is dependent on the particular choice of FEC ( $k_i$ ). For RS codes,  $p_{bk}(k_i)$ , can be defined as,

$$p_{bk}(k_i) = \sum_{j=t(k_i)+1}^n \binom{n}{j} \text{BER}^j (1 - \text{BER})^{n-j} \quad (14)$$

where 'BER' is the bit error rate based on the modulation type and observed SNR ( $\gamma$ ). For a Rayleigh fading channel and M-PSK modulation currently used in IEEE 802.11b systems, this is given as [27],

$$\text{BER} = 1 - \sqrt{\frac{m' \cdot r_c \cdot \gamma \sin^2 \frac{\pi}{M}}{1 + m' \cdot r_c \cdot \gamma \sin^2 \frac{\pi}{M}}} \quad (15)$$

where  $M = 2^{m'}$  gives the order of modulation and  $r_c$  is the rate encoder used.

From the pilot pulses received on its favorable channel, MR  $i$  measures the SNR and derives the bit error rate from Eq. (15). It then chooses a value of the FEC code ( $n - k_i$ ) such that the PER obtained from Eq. (13) is below a pre-decided threshold  $\text{PER}_{th}$ . The final end-to-end latency  $L_\eta$  of the route is hence a function of the choice of the FEC.

#### 3.5.2. FEC influencing goodput

The MR that has the minimum number of useful bits passing through it per unit time, provides an upper bound on the end-to-end performance of the route  $\eta$ . Based on the choice of  $k_i$  that keeps the PER below  $\text{PER}_{th}$  (Eq. (13)) and the analytical calculation of

the hop delay  $T_i^D$  (Eq. (10)) for a given MR  $i$  in the route, the goodput is formally expressed as,

$$G_\eta = \min_{v_i \in H_\eta} \left\{ \frac{\lfloor \frac{L}{n} \rfloor \cdot k_i}{T_i^D} \right\} \quad (16)$$

Here, both the terms are a function of the FEC length and thus, the goodput is strongly dependent on the choice of FEC codes.

### 3.5.3. FEC-routing integration

The above analytical formulations suggest the need for the destination to evaluate the performance constraints, before choosing one of the routes. The necessary information for this is collected in a two stage process. First, the transmitter MR  $i$  sends some local information in the RREQ broadcast, which we call as *sender-specific* fields. These fields are over-written at each hop and are, namely, (i) the favorable channels for MR  $i$  ( $F_i^T$ ), (ii) the number of other contending MRs ( $N_i$ ), and (iii) the current buffer delay ( $T_i^{\text{buf}}$ ) on each of those channels. Based on these values and the measured SNR of the pilot pulses, MR  $j$ , the latter calculates,

1. The preferred transmission channel and rate for MR  $i$ ,
2. The choice of the FEC ( $k_i$ ) for this channel,
3. The total analytical hop delay,  $T_i^D$ , incurred at node  $i$  for this channel.

As the next stage, the values of the FEC ( $k_i$ ) and  $T_i^D$  are included in the fields containing *path information*, that is used by the destination to check the latency and goodput constraints. When an RREP is propagated from the destination to the source confirming the route, the previous hop MR  $j$  includes these fields to allow the previous hop  $i$  to set its transmission parameters.

The protocol description, up to this point, has focussed on the propagation of a single RREQ. The destination may receive multiple copies of the RREQ, and it shortlists one of the available routes as shown next.

### 3.6. Route selection at destination

By deferring the RREQ transmission based on channel quality, a *best effort* attempt is made by XCHARM scheme to create optimal routes. We note that, though classical routing protocols also reinforce the route specified by the earliest arriving RREQ on the CCC, the end-to-end delay in this case is not a true measure of the actual path latency of the channel eventually used for routing.

In order to account for collisions and MAC layer delays that affect the RREQ arrival time, we consider a window period,  $T_w$ . Any incoming request, within a time  $T_w$  of the first arriving RREQ, is placed in the candidate set. The receiver checks if the route  $\eta$  has an analytical path latency ( $L_\eta$ ) and goodput ( $G_\eta$ ) that meets the performance thresholds,  $L_{\eta_{th}}$  and  $G_{\eta_{th}}$ , respectively. This is accomplished with the help of the information in the RREQ and the Eqs. (9) and (10). Thus, the chosen route  $\eta_{opt}$  satisfies the constraints,

$$\eta_{opt} = \{ \eta | L_\eta < L_{\eta_{th}} \& G_\eta > G_{\eta_{th}} \} \quad (17)$$

Here, we undertake a simple procedure of choosing the first route that keeps the end-to-end latency within the threshold ( $L_\eta < L_{\eta_{th}}$ ) and the observed goodput above the minimum limit ( $G_\eta > G_{\eta_{th}}$ ). If the latency and goodput conditions are not jointly satisfied for any of the candidate RREQs, the route with the least latency is arbitrarily chosen. An RREP packet is now sent along the chosen route that confirms their participation of the MRs.

The channel assignment is static for a given link as long as the end to end performance constraints are met. Else, the channel assignment may be revisited through the route management scheme described in Section 3.7. Additionally, two nodes that have

an ongoing communication may potentially serve as part of a new route. When such an actively communicating pair receives a new RREQ packet, it skips the Channel and MR ranking step (as the channel state is known), and directly goes into the stage of forwarding the RREQ with a delay based on the rank of the already chosen channel. The rest of the route formation steps remain the same, for the final route is chosen by the destination by considering different arriving RREQs, based on whether this particular set of constituent links of the route meets the specified end to end constraints.

### 3.7. Route management

We define *soft* and *hard* route recovery as follows, in cases of an increase in the external interference, changes in the fading environment or subsequent involvement in multiple routes that may cause higher link delay and possibly violate the end-to-end thresholds.

#### 3.7.1. Soft recovery

XCHARM first attempts to discover a new route from the point of failure, i.e., if the MR  $\mu$  reports a significant change in its network environment, a route error (RERR) is sent by the destination to the previous hop MR  $\mu - 1$  on that route. The latter now initiates the formation of a new route by sending out an RREQ. The previous route is kept in operation till the new one is chosen and an RREP is sent by the destination confirming it. At the same time, a route tear-down message (RTEAR) is sent in the earlier route freeing the MRs.

#### 3.7.2. Hard recovery

If (i) the affected MR  $\mu$  cannot be identified or (ii) no feasible route is found after the soft recovery stage or (iii) no RREQ is heard from the MR  $\mu - 1$ , the destination sends the RERR back to the source signaling the need of a completely new route.

A key component of the route management scheme is the identification of the point of failure. Each MR  $i$  maintains an average value of the observed total hop delay  $T_i^D$  which is compared with the last communicated value to the destination. If the deviation between the two is greater than a pre-decided constant, the new value of  $T_i^D$  (say,  $T_i^{D'}$ ) is piggybacked on the data packets to the destination. If the current route does not satisfy the constraints in Eq. (17), the affected MR  $\mu$  is identified, with high probability, by simply checking the highest link delay as  $\mu = \arg_i \max\{T_i^D\}$ .

The two levels of recovery attempt to balance the promptness in the response of the system to a change in the environment and the consumption of the network resources in the process.

## 4. Performance evaluation

In this section, we evaluate the performance of the proposed cross-layer protocol. We first describe the basic simulation setup in Section 4.1. Sections 4.2 and 4.3 study the benefits of the channel selection scheme and the improvement obtained with the rank based path latency respectively. The effect of the end-to-end constraints on our proposed algorithm, the FEC optimization, and route recovery are demonstrated in Section 4.4. Section 4.5 evaluates the overhead introduced by our scheme in terms of routing load, route setup latency and protocol-specific metrics.

### 4.1. Simulation setup

XCHARM is implemented in NS-2 by first extending it to a multi-radio, multi-channel environment. A multi-path Rayleigh environment was setup in MATLAB and imported for each random

node topology used for simulation. We placed 20 obstacles in an area of  $1000 \times 1000 \text{ m}^2$  and for every pair of MRs, we calculated the ray propagation paths based on reflections from these obstacles. The reflection coefficient was set at 0.9. The coherence bandwidth  $B_c$  of the channel in the 2.4 GHz band was set at 260 kHz, considering an urban area with high-rise buildings, from the experimentally derived values in [21]. The bit error rates for the flat and frequency selective fading channels are then respectively applied from the results shown in Fig. 2(a).

The spectral overlap factor  $I$  for IEEE 802.11b is given in [13]. A default value noise value of  $-100 \text{ dBm}$  is considered for each receiver. We adapted the IEEE 802.11b link layer to allow  $\psi = 4$  different transmission rates (also channel/MR ranks), 1, 2, 5 and 10 Mbps. The packet and the block sizes are fixed at 1024 and 128 bytes, respectively. For the QPSK modulation used at each rate, the parameters in Eq. (15) are set as  $M = 4$ ,  $m' = 2$ . Unless specified otherwise, the values of the simulation parameters are shown in Table 1.

We consider three scenarios in our study (i) *random* topology, in which 50 MRs are uniformly distributed in the area, (ii) *parallel* topology, which consists of two chains of MRs as shown by the encircled region in Fig. 5, and the (iii) *row* topology, formed by MRs 0–12 in Fig. 5. The *parallel* and *row* topologies are chosen, in some selected experiments, to highlight certain key aspects of our protocol. All the other results are for the general case of randomly deployed MRs.

#### 4.2. Effect of channel selection

In order to evaluate our interference based channel selection model proposed in Section 3.2, the effects of the channel ranking mechanism, the link FEC code assignment and the transmit rate adaptation are disabled. All the MRs in random topology transmit with a fixed rate of 2 Mbps.

1. AODV: The single-radio single-channel routing algorithm proposed in [25] is evaluated. One route is discovered and utilized for data packets transmission.
2. AODV-MR: The multi-radio multi-channel extension of AODV proposed in [26] is evaluated. Channel allocation is performed during the route discovery phase.
3. LMR: The multi-radio multi-channel protocol described in [22] is evaluated. Channel allocation is performed during the route discovery phase, attempting to balance the traffic load of each channel [22].

Unless specified otherwise, each MR can transmit on 11 channels, and is equipped with an equal number of transceivers.

In Fig. 6 we show the performance results of the four protocols in a scenario with 3 active connections, where we vary the connection load produced by each connection (from 150 Kb/s up to 1 Mb/s). Fig. 6(a) shows the average end-to-end goodput in such a scenario. From Fig. 6(a) shows AODV with a goodput lower than 200 Kbps due to its single-radio architecture. Also, LMR experiences higher goodput than AODV-MR when the connection load increases. However, both AODV-MR and LMR do not account for spectral leakage interference caused by MRs that transmit on non-orthogonal channels. As a result, XCHARM provides a considerable performance improvement under high connection loads (e.g.,  $\geq$  than 400 Kb/s). The ability of our scheme to maximize channel re-use and to reduce inter-flow interference under heavy traffic load conditions is also shown in Fig. 6(b) for the packet delivery ratio (PDR). Fig. 6(c) shows the average end-to-end delay with XCHARM demonstrating the best performance in all the traffic load configurations.

**Table 1**  
Simulation parameters.

Simulation tools	Ns2, Matlab
Network area	Square of $1000 \times 1000 \text{ m}^2$ with 20 obstacles
Propagation model	Ray-tracing model
Network topologies	Random (50 MRs), Parallel, Row
Transmitting range	240 m
Transmitting rate	{1, 2, 5, 10} Mbps
Max defer timer ( $T_{\max}^{\text{def}}$ )	0.2 s
Power threshold ( $P_{th}$ )	$-75 \text{ dBm}$
Packet error rate threshold ( $\text{PER}_{th}$ )	0.2
Waiting time threshold ( $T_w$ )	1 s
MAC protocol	IEEE 802.11 DCF
Traffic type	UDP-CBR (Constrant Bit Rate)
Packet size	1024 Bytes
Connection load	{100, 250, 400, 550, 700, 850, 1000, 1150} Kbps
Number of connections	{1, 8}
Number of channels	{5, 7, 9, 11}
Number of radio	{5, 7, 9, 11}
Number of simulation runs	30

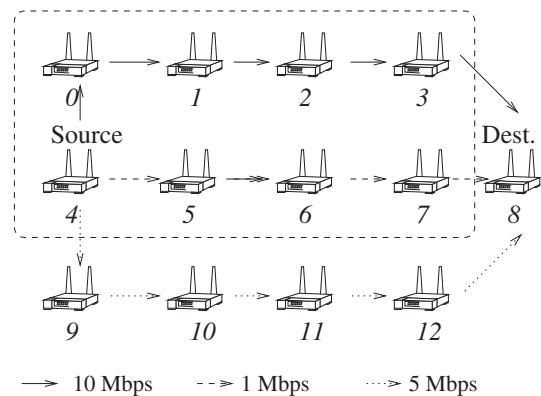


**Fig. 5.** The parallel and row topologies.

In Fig. 7(a), (b) and (c), we vary the number of active connections. Each connection transmits data with a constant rate (e.g., 500 Kb/s). Fig. 7(a) shows the average end-to-end goodput, where in more flows increase the average contention of each channel due to interference and spectral leakage caused by nodes using adjacent channels [13]. The single-channel AODV gets saturated first. AODV-MR also suffers interference caused by nodes transmitting in the same channel or in adjacent channels. Both XCHARM and LMR protocols perform interference-aware channel selection, and thus scale well when the number of connections increase. The XCHARM architecture obtains a goodput performance substantially higher than AODV, AODV-MR and LMR. The same improvement can be seen in terms of end-to-end delay, which is shown in Fig. 7(b) and and in terms of packet delivery ratio, which is shown in Fig. 7(c).

In Fig. 8(a) and (b), we evaluate the impact of the number of channels on the end-to-end performance in the Random scenario with a constant network load (3 active flows). As expected, no appreciable difference can be observed between the XCHARM and AODV-MR and LMR when the number of available channels is low (5). However, as the number of channels increases ( $>5$ ), the XCHARM allocation scheme is able to reduce the conflicts among neighboring nodes, because it attempts to allocate interfering nodes on different channels. This translates in reduced end-to-end delay in accessing the channel (Fig. 8(a)), as well as lower packet loss due to MAC contention (Fig. 8(b)), and higher end-to-end goodput (Fig. 8(c)).

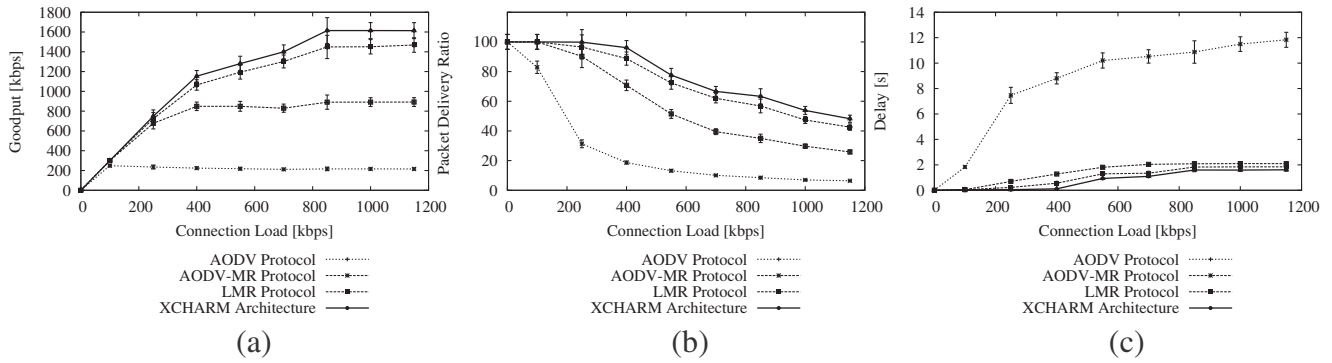


Fig. 6. For the Random topology, the system goodput (a), the packet delivery ratio (b) and the end-to-end delay (c) are shown, as a function of the connection load.

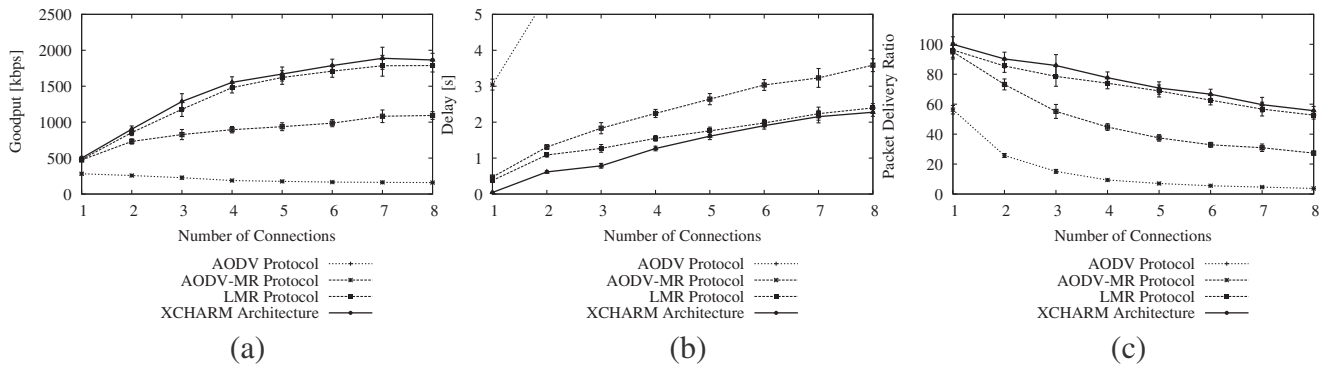


Fig. 7. For the Random topology, the system goodput (a), the end-to-end delay (b) and the packet delivery ratio (c) are shown, as a function of the number of active connections.

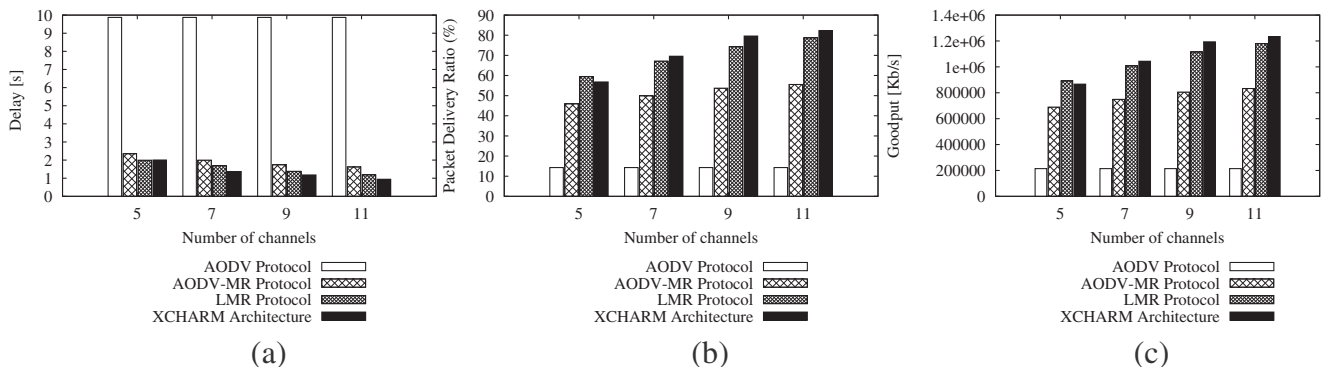


Fig. 8. The impact of the number of channels on the end-to-end delay, packet delivery rate and goodput are shown in (a), (b) and (c), respectively.

### 4.3. Effect of MR ranking and initiative

In this section, we enable the effects of the defer timer (DT), of the channel ranking (CR) and of the transmit rate adaption on XCHARM. More specifically, we consider three different XCHARM configurations, based on the usage of CR and/or DT:

- XCHARM (CR = off, DT = off): the resulting scheme neither accounts for channel interference (as CR = off) nor the fading environment (and hence, the transmission rate) (as DT = off). However, we incorporate the automatic rate selection (ARS) scheme at the link layer to provide a packet error recovery mechanism typically used in commercial IEEE 802.11b systems.
- XCHARM (CR = on, DT = off): the ranking scheme described in Section 3.3 is used, but without the defer delay on RREQs based on channel rank (Section 3.4).

- XCHARM (CR = on, DT = on): the full XCHARM scheme is implemented, with the channel ranking and the defer timer mechanisms always enabled.
- XCHARM Least Latency: the best routes providing the lowest end-to-end transmission delay are used, by means of a centralized approach (i.e., the Dijkstra algorithm) to set the upper bound in terms of optimal channel selection.

We observe from Fig. 9(b) that the route formed by the full configuration (CR = on, DT = on) experiences about half the end-to-end delay as the one with the DT disabled, and this difference increases with the number of flows. The configuration with CR disabled experiences the highest end-to-end delay, as it is affected by frequency selective fading. Moreover, when the DT is enabled, the route with the higher allowed transmission rates (based on fading) delivers the RREQs message earlier, showing improvement in Fig. 9(b). As the

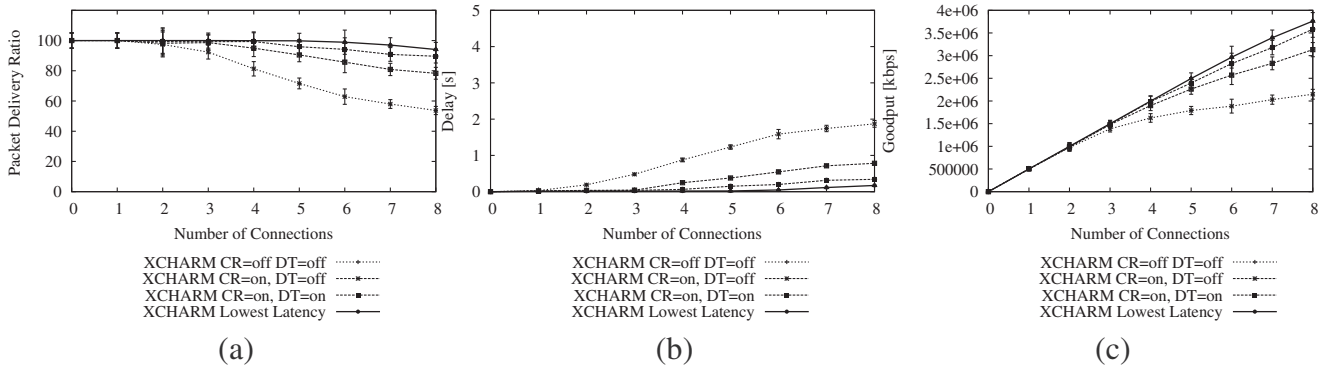


Fig. 9. For the Random topology, the PDR (a), the end-to-end latency (b) and the system goodput (c) are shown. Choosing routes considering the fading environment and the transmission rate results in significant improvement for all the metrics.

performance of the full XCHARM scheme is close to the XCHARM Least Latency configuration, this confirms the operation of the channel rank (Section 3.3) and and defer function (Section 3.4) in a distributed environment. The quality of the chosen route can be measured by the packet delivery ratio (PDR), as shown in Fig. 9(a). Although all three configurations experience a drop in the PDR with increased network load, not considering fading may result in a considerable poor performance, as is seen for the case (CR = off, DT = off). Fig. 9(c) shows the improvements introduced by the full XCHARM configuration in terms of end-to-end goodput, which is close to the upper bound.

#### 4.4. Route maintenance

In this section, we show how XCHARM meets the end-to-end performance constraints of latency and goodput, described in Section 3.6. For this test, we use the Row topology, with the maximum transmission rate allowing flat fading links, as shown in Fig. 5. This topology allows us to study clearly the route choices made by our routing scheme with all the individual optimization modules enabled. We consider the three paths:  $P_1 = \{4 - 5 - 6 - 7 - 8\}$ ,  $P_2 = \{4 - 0 - 1 - 2 - 3 - 8\}$  and  $P_3 = \{4 - 9 - 10 - 11 - 12 - 8\}$ . We consider an application with

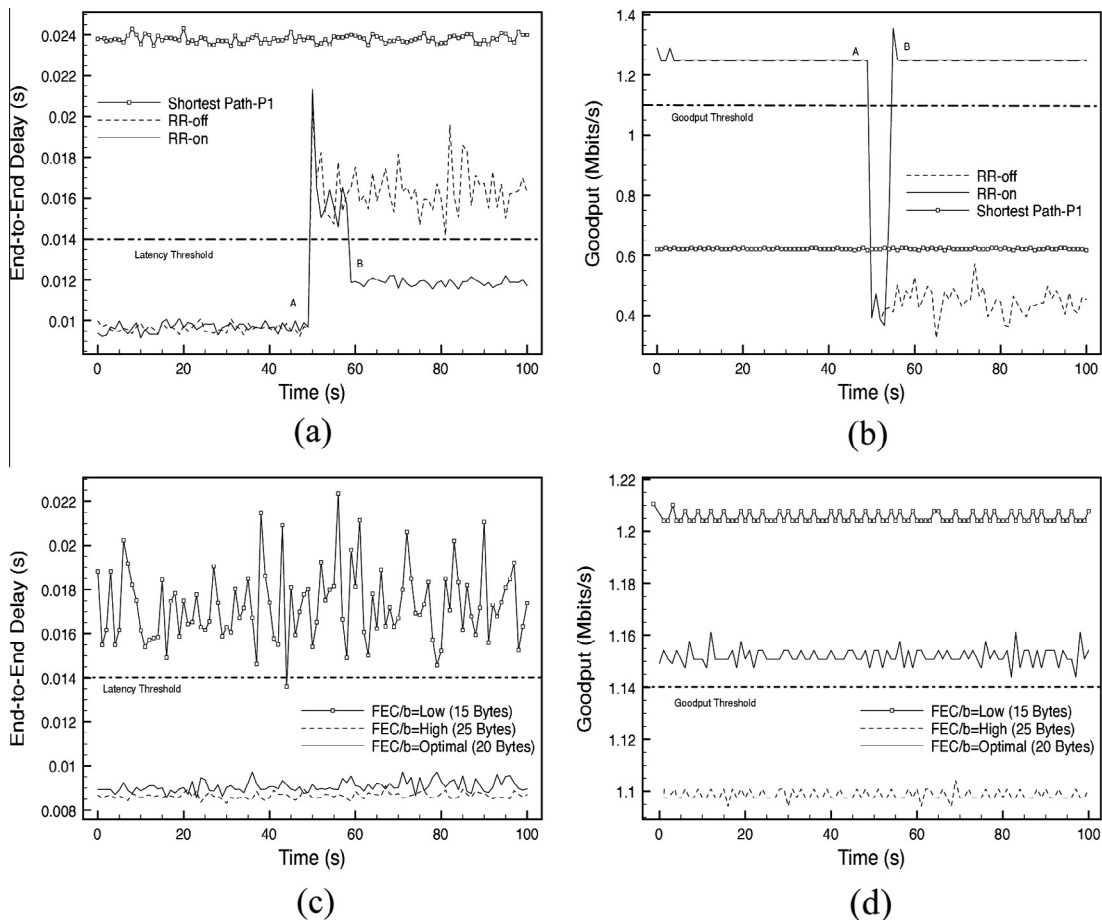
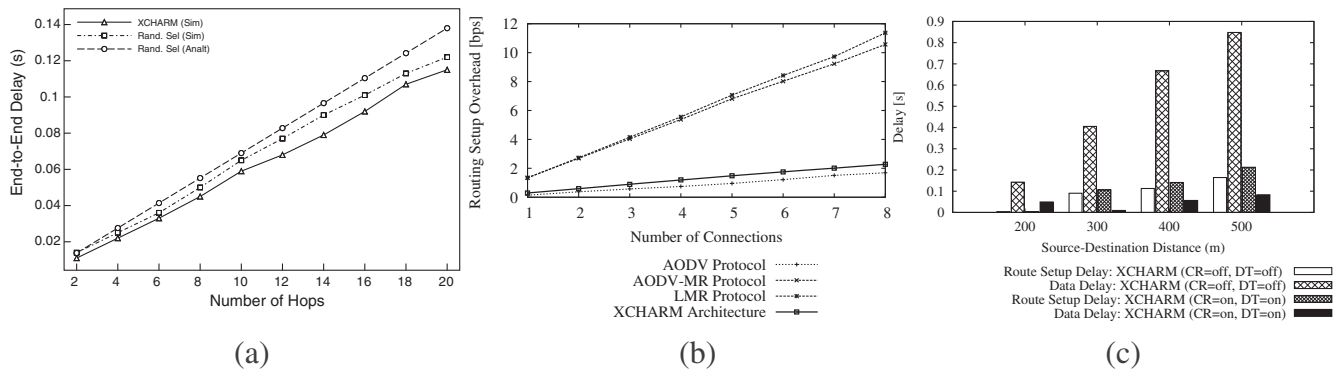


Fig. 10. The working of the route management function for the path latency and goodput constraints is shown in (a) and (b) respectively when the route recovery module is disabled (RR-off) and enabled (RR-on). The effect of the choice of FEC is shown in (c) and (d).



**Fig. 11.** The overhead of the route setup phase of our proposed is shown with respect to the bits transmitted per MR in (a). The overall latency, of the route setup and operation, is shown in (b).

these constraints of latency and goodput:  $L_{Th} = 0.014$  s and  $G_{Th} = 1.14$  Mbps.

In the classical approach, the shortest route  $P_1$  is preferred as it involves the fewest hops and the RREQ, propagating over the CCC, reaches the destination first. However, the data passing through this route experiences an unacceptably large end-to-end delay, as the true channel conditions (and hence the maximum transmission rate) were not captured by the RREQ. XCHARM chooses the longer route  $P_2$ , as the RREQ experiences a lower forwarding delay based on the ranking concept. After 50 s of simulation (marked by A in Fig. 10(a)), another bi-directional flow is created between the MRs 1 and 2. This results in increased buffer delay and channel access times for these MRs, thus raising the end-to-end latency beyond the acceptable limit.

We repeat this experiment with the goodput metric in Fig. 10(b) by increasing the noise power on links 0–1 and 1–2 to  $-80$  dBm. The resulting packet loss reduces the useful bits received per second at the destination below the threshold, signaling the formation of a new route  $P_3$  that meets the user constraints.

Figs. 10(c) and (d) show the need for analytically deciding an optimal value of the FEC code. We consider the row topology described above, with 1 active flow between the MRs 4 and 8 on route  $P_1$ . Each link of the route experiences a constant PER due to fading. First, we consider the case in which the size of the FEC code per block is pre-decided to a minimum and maximum value, i.e., to  $n - k = 25$  bytes and 15 bytes, without considering the performance requests of the application. For a FEC size of 25 bytes, we observe that the end-to-end latency requirement is satisfied, but not the goodput constraint. Adapting the per-block FEC to 20 bytes based on PER conditions at each link, XCHARM is able to meet both the delay and goodput constraints.

Fig. 11(a) shows the end-to-end latency as a function of the length of each route for the Parallel topology. Here, the maximum number of interfering neighbors for each MR is 5. We also plot the analytical end-to-end delay by summing the link latencies obtained from Eq. (10). Our estimate closely matches the simulation results as a demonstration that this formulation is suitable for matching the performance guarantees at the destination.

#### 4.5. Overhead analysis

Fig. 11(b) shows the routing overhead for path setup. Here, AODV requires the lowest routing overhead rate. XCHARM protocol introduces comparatively higher overhead, caused by: (i) the multi-hop forwarding of CCONF messages, and (ii) the additional information conveyed by the RREQ. However, Fig. 11(b) shows that such an overhead is still lower than that experienced by AODV-MR and LMR protocols, where each RREQ message is re-broadcast on all the

available radio interfaces. A similar trend is seen in Fig. 11(c) in the route setup time, measured as a function of the source–destination distance. XCHARM, with CR and DT disabled, no longer introduces a channel-quality based delay in the CCC. The route setup time is combined with the actual end-to-end latency of the operational route in Fig. 11(c). We observe that the full XCHARM scheme (CR = on, DT = on) introduces an additional delay on route setup caused by the defer timer (Section 3.4), which is compensated by the lower end-to-end latency for routes with better channel fading conditions.

## 5. Conclusions

In this paper, we have presented XCHARM, a multi-channel, multi-radio cross-layer routing protocol for WMNs that accounts for interference based channel assignment and fading effects. Our routing protocol attempts to provide an end-to-end performance guarantee before the route is actually used based on an analytical formulation of the links delays. While the work in this paper is geared towards 802.11b networks, other advanced flavors such as a/g/n use OFDM with extremely small subcarrier bandwidths. In such cases, there are two critical considerations: first, whether each subcarrier can be tested for frequency selective behavior, and whether such fine grained analysis yields sufficient cost-benefit tradeoffs. The time granularity at which the pulses can be sent provide the lower bound on the determination of the coherence bandwidth (at least, they must be comparable to the subcarrier bandwidth). Moreover, determining the coherence bandwidth for over dozens of subcarriers, almost instantaneously may be prohibitively computationally expensive. We believe a phased approach, where selected subcarrier-groups are chosen for testing the fast fading condition is better suited, though this will be investigated in our future research.

## References

- [1] IEEE Std 802.11b-1999/Cor 1-2001, 2001.
- [2] D. Aguayo, J. Bicket, S. Biswas, G. Judd, R. Morris, Link-level Measurements from an 802.11b Mesh Network, in: Proceedings of ACM SIGCOMM, Portland, Oregon, USA, 2005, pp. 121–132.
- [3] A.M. Akhtar, M.R. Nakhai, A.H. Aghvami, Power aware cooperative routing in wireless mesh networks, *IEEE Communications Letters* 16 (5) (May 2012) 670–673.
- [4] I.F. Akyildiz, X. Wang, W. Wang, *Wireless mesh networks: a survey*, *Elsevier Computer Networks Journal* 47 (4) (Nov. 2005) 445–487.
- [5] M. Alicherry, R. Bhatia, L. Li, Joint channel assignment and routing for throughput optimization in multi-radio wireless mesh networks, in: Proceedings of ACM MobiCom, Germany, 2005, pp. 58–72.
- [6] A. Bezzina, M. Ayari, R. Langar, F. Kamoun, An interference-aware routing metric for multi-radio multi-channel wireless mesh networks, in: Proceedings of IEEE WiMob, 8–10 Oct. 2012, pp. 284–291.

- [7] G. Bianchi, Performance analysis of the IEEE 802.11 DCF, *IEEE Journal on Selected Areas of Comm.*, 18 (3) (2000) 535–547.
- [8] K. Chowdhury, M. Di Felice, L. Bononi, A fading and interference aware routing protocol for multi-channel multi-radio wireless mesh networks, in: *Proceedings of ACM International Symposium on Performance Evaluation of Wireless ad Hoc, Sensor and Ubiquitous Networks (PE-WASUN)*, Spain, October 2009, pp. 1–8.
- [9] M.E. Campista, P.M. Esposito et al., Routing metrics and protocols for wireless mesh networks, *IEEE Network* 26 (1) 22 (1) (2008) 6–12.
- [10] D. Chafekar, V.S.A. Kumar, M.V. Marathe, S. Parthasarathy, Aravind Srinivasan, Cross-layer latency minimization in wireless networks with SINR constraints, in: *Proceedings of ACM MobiHoc*, Montreal, Quebec, Canada, 2007, pp. 110–119.
- [11] P. Chatzimisios, A.C. Boucouvalas, V. Vitsas, Influence of channel BER on IEEE 802.11 DCF, *IEEE Electron. Lett.* 39 (23) (2003) 1687–1689.
- [12] L. Chen, S.H. Low, M. Chiang, J.C. Doyle, Cross-layer congestion control, routing and scheduling design in ad hoc wireless networks, in: *Proceedings of IEEE INFOCOM*, Spain, 2006, pp. 1–13.
- [13] K.R. Chowdhury, I.F. Akyildiz, Cognitive wireless mesh networks with dynamic spectrum access, *IEEE J. Selected. Areas Commun.* 26 (1) (2008) 168–181.
- [14] L. Dai, Y. Xue, B. Chang, Y. Cao, Y. Cui, Integrating traffic estimation and routing optimization for multi-radio multi-channel wireless mesh networks, in: *Proceedings of IEEE INFOCOM*, Phoenix, AZ, USA, 2008, pp. 502–510.
- [15] Y. Ding, K. Pongaliur, L. Xiao, Channel allocation and routing in hybrid multichannel multiradio wireless mesh networks, *IEEE Trans. Mobile Comput.* 12 (2) (Feb. 2013) 206–218.
- [16] T. ElBatt, T. Andersen, Cross-layer interference-aware routing for wireless multi-hop networks, in: *Proceedings of the International Conference on Wireless Comm. and Mobile Comp.*, New Orleans, Vancouver, British Columbia, Canada, USA, 2006, pp. 153–158.
- [17] D. Gokhale, S. Sen, K. Chebrolu, B. Raman, On the feasibility of the link abstraction in (rural) mesh networks, in: *Proceedings of IEEE INFOCOM*, Phoenix, AZ, USA, 2008, pp. 484–492.
- [18] A. Goldsmith, *Wireless Communications*, first ed., Cambridge University Press, 2005.
- [19] Michelle X. Gong, Scott F. Midkiff, Shiwen Mao, A cross-layer approach to channel assignment in wireless ad hoc networks, *Mobile Network. Appl.* 12 (1) (2007) 43–56.
- [20] A. Kashyap, S. Sengupta, R. Bhatia, M. Kodialam, Two-phase routing, scheduling and power control for wireless mesh networks with variable traffic, in: *Proceedings of ACM SIGMETRICS*, San Diego, California, USA, 2007, pp. 85–96.
- [21] A.H. Kemp, E.B. Bryant, Channel sounding of industrial sites in the 2.4 GHz ISM Band, *Wireless Personal Commun.* 31 (3–4) (2004) 235–248.
- [22] A.N. Le, D.W. Kum, Y.Z. Cho, Load-aware routing protocol for multi-radio wireless mesh networks, in: *Proceedings of IEEE ICCE*, San Diego, USA, 2006, pp. 138–143.
- [23] A. Mishra, V. Shrivastava, S. Banerjee, W. Arbaugh, Partially overlapped channels not considered harmful, *ACM SIGMETRICS Perform. Eval. Rev.* 34 (1) (2006) 63–74.
- [24] D. Passos, C.V.N. Albuquerque, A joint approach to routing metrics and rate adaptation in wireless mesh networks, *IEEE/ACM Transactions on Networking* 20 (4) (Aug. 2012) 999–1009.
- [25] C.E. Perkins, E.M. Belding-Royer, Ad hoc on demand distance vector (AODV) routing, in: *Proceedings of IEEE WMCSA*, New-Orleans, USA, 1999, pp. 90–100.
- [26] A.A. Pirzada, M. Portmann, J. Indulska, Evaluation of multi-radio extensions to AODV for wireless mesh networks, in: *Proceedings of ACM MobiWac*, Terromolinos, Spain, 2006, pp. 45–51.
- [27] D. Yuan, L. Zhang, C. Gao, Performance analysis of RS-BCH concatenated codes in Rayleigh fading channel, in: *Proceedings of Asia-Pacific Conference on Commun.* 3(1) (2009) 315–325.